

Strong-correlation effects in Born effective charges.

Alessio Filippetti and Nicola A. Spaldin

Materials Department, University of California, Santa Barbara, CA 93106-5050

Large values of Born effective charges are generally considered as reliable indicators of the genuine tendency of an insulator towards ferroelectric instability. However, these quantities can be very much influenced by strong electron correlation and metallic behavior, which are not exclusive properties of ferroelectric materials. In this paper we compare the Born effective charges of some prototypical ferroelectrics with those of magnetic, non-ferroelectric compounds using a novel, self-interaction free methodology that improves on the local-density approximation description of the electronic properties. We show that the inclusion of strong-correlation effects systematically reduces the size of the Born effective charges and the electron localization lengths. Furthermore we give an interpretation of the Born effective charges in terms of band energy structure and orbital occupations which can be used as a guideline to rationalize their values in the general case.

PACS numbers: Valid Pacs

I. INTRODUCTION

Following the implementation of the linear-response theory¹ and the Berry phase approach^{2,3} to the electron polarization within the local-spin density approximation (LSDA), there has been tremendous progress in understanding the properties of piezoelectric and ferroelectric materials from a microscopic standpoint. Indeed, spontaneous polarization, piezoelectric constants, and Born effective charges (BEC), as well as full phonon spectra and potential energy surfaces can be calculated from first-principles giving thus a detailed picture of the electronic and structural behavior.

The Born effective charges (BEC), i.e. the change in electron polarization upon ionic displacements, are the main subject of this paper. They play an important role in the physics of ferroelectric and even piezoelectric materials, since they contribute to the LO-TO phonon frequency splitting at Γ (which is characteristically large in ferroelectric materials⁵) and to the piezoelectric tensor.⁶ Furthermore, the behavior of the BEC is highly non-trivial since it is related to the microscopic electron current produced in a system by a change of the atomic position.⁴ This current may give a contribution to the BEC which is unrelated and additional to the static electron charge carried by the ion during the displacement, so that the BEC can be much bigger than their static counterpart. In this case the BEC are usually referred to as anomalous.

Interestingly, the BEC are found to be highly anomalous in the high-temperature (i.e. centrosymmetric) phase of many ferroelectric compounds. In particular, they are anomalous for the whole family of ferroelectric perovskites,^{5,7,8,9,10} and for the class of IV-VI chalcogenides,¹¹. Since both the BEC anomaly and the mechanism of the ferroelectric phase transition in most of the ferroelectric perovskites can be related to the hybridization of anion p and cation d orbitals^{7,12,13}, the in-

teresting hypothesis arises that a large value of the BEC might be an indicator of the ferroelectric materials, or materials which are on the verge of a ferroelectric transition. However, according to recent calculations the BEC do not appear to possess such a predictive capability in general. On one hand they are found to be anomalous in a magnetic perovskite (CaMnO_3 ¹⁴) which is far from ferroelectric. On the other hand they are non-anomalous in the ferromagnet YMnO_3 , which belongs to the family of the hexagonal manganese oxides^{15,16,17}, whose ferroelectric transition is driven not by chemical activity (e.g. anion-cation hybridization changes) but by structural collapse and oxygen rotations.¹⁸

So we see that the meaning of the BEC and origin of the anomalous part are far from being completely clarified. While the role of covalent bonding in favoring spontaneous polarization and large BEC in ferroelectric perovskites is well understood,^{7,9,13} other aspects which can strongly influence the values of the BEC, like the metallic character and the strong electron correlation correlation, have been scarcely investigated so far.

In an insulator on the verge of an insulating-to-metal transition, the BEC can diverge to anomalously large values, thus indicating an electron current which can freely flow through the system in response to the electric field associated with an ionic displacement.¹¹ Even more interesting is the effect of strong electron-correlation. In a series of papers Ishihara and co-workers¹⁹ showed that in a two-band, Hubbard model, the introduction of strongly-correlated effects (namely the on-site Coulomb energy) induces a strong enhancement of the electron-phonon coupling which becomes divergent at the transition boundary from the weakly-correlated (small U) to the strongly-correlated regime (large U). Resta and Sorella²⁰ showed that, in the same model, in the region of the transition boundary, the BEC are divergent and undergo a sign change (i.e. the electron current changes its direction flowing from the cation to the anion) for

large U .

Later the same authors introduced the concept of electron localization length²¹ (λ) as a measure to discriminate between the metallic regime (where $\lambda=\infty$) and the insulating regime. Within the same Hubbard model, they found that the BEC and λ diverge simultaneously for the same value of U (i.e. the BEC diverge in the metallic state),

Despite these predictions from model Hamiltonians, to our knowledge very few attempts have been made to calculate these properties for strongly-correlated materials from first-principles. The main reason is likely the questionable reliability of LSDA calculations for describing the electronic properties of strongly localized, atomic-like, electron states. It is common knowledge, indeed, that the LSDA is often inaccurate in describing these systems.^{22,23} However, there is increasing evidence that many of the LSDA failures are not due to the lack of genuine many-body electron correlation, but rather to the presence of the spurious self interaction (SI) within the LSDA functional,²² which becomes particularly strong for spatially localized electron charges. The effects of the SI were first studied by Perdew and Zunger²² on atoms. Subsequently Svane and co-workers²⁴ implemented a self-interaction-corrected (SIC) scheme for extended systems, obtaining large improvements over the LSDA results for the electronic properties of transition metal oxides and high- T_c superconductors. However their method was not simple and general enough to be extensively applied to a vast range of systems, thus the capabilities and the performance of the SIC remained largely untested.

Recently we developed a self-interaction free pseudopotential scheme (pseudo-SIC)²⁵ based on the idea (originally conceived by Vogel and co-workers²⁶) of expressing the SI as a non-local, pseudopotential-like projector. This approach has the advantage of being applicable to a vast generality of systems including semiconductors and metals, magnetic and non magnetic materials, without requiring large modifications or a large increase of computing effort with respect to the usual LSDA. The pseudo-SIC is close in spirit to the popular LDA+ U ^{27,28} since removing the SI is analogous to effectively mapping the on-site energy U into the one-electron picture, so that both weakly-correlated materials and Mott-insulators can be treated on the same foot. In Ref.25 we showed that the method is accurate in describing the band energies of III-V and II-VI semiconductors (e.g. GaN and ZnO), transition metal monoxides (NiO, MnO) and hexagonal ferroelectrics (YMnO₃).

In this paper we apply the pseudo-SIC to the study of the BEC for a range of different materials including a prototypical ferroelectric perovskite (BaTiO₃), a ferroelectric with extremely high BEC (GeTe), a magnetic perovskites (CaMnO₃) and two magnetic monoxides (MnO and NiO). This investigation aims to furnish

a more complete and accurate picture of the BEC, and to spread light on the meaning of their anomalous values.

We show that the BEC anomaly is not a property of ferroelectric materials, but is instead present in ionic insulators whenever the energy difference between filled anion and empty cation bands is particularly small (less than 3 eV), or in materials with nearly metallic behavior. Furthermore, we give evidence that the effect of strong correlation systematically reduces the value of the BEC and of the electron localization length. This decrease is particularly evident for the BEC which are described as highly anomalous within LDA (or LSDA). Thus, part of (but not all) the BEC anomaly found within LDA is a consequence of the unphysical self-interaction which overemphasizes the orbital hybridization and the sensitivity of the electron-phonon coupling to the atomic displacement.

Finally, we propose an interpretation of the BEC in terms of occupation and capacity of the filled and empty orbitals, respectively, which allows a qualitative understanding of the anomaly in a general case.

The remainder of the paper is organized as follows: in Section II we briefly illustrate the pseudo-SIC scheme, and the formulation used for the BEC calculation. Section III is devoted to the presentation and the discussion of our results, and in Section V we give our final remarks.

II. FORMULATION

A. Self-interaction corrected approach

Here we briefly summarize the main features of the pseudo-SIC approach. A detailed discussion of the formalism and the assumptions which are at the basis of this method can be found in Ref. 25. The formalism uses ultrasoft pseudopotentials (USPP²⁹) which give optimal transferability and require low cut-off energies even for transition metal atoms. The SI-free, Kohn-Sham equations are:

$$\left[-\nabla^2 + \hat{V}_{\text{pp}} + \hat{V}_{\text{hxc}}^\sigma - \hat{V}_{\text{sic}}^\sigma\right] |\psi_{n\mathbf{k}}^\sigma\rangle = \epsilon_{n\mathbf{k}}^\sigma |\psi_{n\mathbf{k}}^\sigma\rangle, \quad (1)$$

where \hat{V}_{pp} is the non-local pseudopotential, V_{hxc}^σ the screening potential, and $\hat{V}_{\text{sic}}^\sigma$ the SIC term. This is expressed as a fully-non local, Kleinman-Bylander-type, pseudopotential projector:

$$\hat{V}_{\text{sic}}^\sigma = \frac{1}{2} \sum_i \frac{|V_{\text{hxc}}^{\sigma i} \phi_i\rangle p_i^\sigma \langle \phi_i V_{\text{hxc}}^{\sigma i} |}{\langle \phi_i | V_{\text{hxc}}^{\sigma i} | \phi_i \rangle} + \frac{1}{2} \sum_{i,\nu,\mu} |\beta_\nu\rangle p_i^\sigma \int d\mathbf{r} V_{\text{hxc}}^{\sigma i}(\mathbf{r}) Q_{\nu\mu}(\mathbf{r}) \langle \beta_\mu|. \quad (2)$$

Here i is a composite index which runs over angular quantum numbers and atomic positions, $\phi_i(\mathbf{r})$ are atomic pseudowavefunctions, $V_{\text{hxc}}^{\sigma i}(\mathbf{r})$ are the SI potentials of the fully occupied spin-polarized atomic pseudocharges $\phi_i(\mathbf{r})^2$, and p_i^σ are the corresponding occupation numbers. The second term in Eq. 2 is the augmented contribution required if using USPP ($\beta_\mu(\mathbf{r})$ and $Q_{\nu\mu}(\mathbf{r})$ are projector functions and augmented charge densities,²⁹ respectively), whereas for ordinary norm-conserving pseudopotentials only the first term in Eq. 2 has to be considered.

All the ingredients needed in Eqs.2 are atomic quantities (thus they are calculated during the initialization), except the occupation numbers, p_i^σ , which must be evaluated self-consistently by projecting the Bloch state manifold onto the pseudoatomic basis:

$$p_i^\sigma = \sum_{n\mathbf{k}} f_{n\mathbf{k}}^\sigma \langle \psi_{n\mathbf{k}}^\sigma | \phi_i \rangle \langle \phi_i | \psi_{n\mathbf{k}}^\sigma \rangle \times \left[1 + \sum_{\nu\mu} \langle \phi_i | \beta_\nu \rangle q_{\nu\mu} \langle \beta_\mu | \phi_i \rangle \right]. \quad (3)$$

Again, the second term of Eq. 3 is only present for USPP. (The augmented charges $q_{\nu\mu}$ are integrals of $Q_{\nu\mu}(\mathbf{r})$.)

B. Electron polarization and localization

For the calculation of the BEC we employ the compact formulation developed by Resta³⁰, which is based on the concept of position operator. This has the advantage of introducing electronic polarization and electron localization length as two quantities steaming from the same source. Here we describe the formulation for spin-polarized systems and USPP which, to our knowledge, has not been presented previously.

The source of the theory is the expectation value z_α of the many-body phase operator:

$$z_\alpha = \langle \Psi_0 | e^{i\Delta\mathbf{k}_\alpha \cdot \hat{\mathbf{R}}} | \Psi_0 \rangle. \quad (4)$$

Here α is the cartesian coordinate, $\hat{\mathbf{R}} = \sum_{i=1}^N \mathbf{r}_i$ the many-body position operator, Ψ_0 the ground-state wavefunction, and $\Delta\mathbf{k}_\alpha$ a reciprocal-space vector of magnitude:

$$|\Delta\mathbf{k}_\alpha| = \frac{2\pi}{L_\alpha} \frac{1}{M}. \quad (5)$$

Here L_α and M are length and number of unit cells (that is number of grid points in reciprocal space) in the α direction, respectively.

Resta showed that the expected value of the position operator, within periodic boundary conditions (PBC), must be calculated as:

$$\langle r_\alpha \rangle = \frac{1}{NG_\alpha} \text{Im} \ln z_\alpha, \quad (6)$$

where $G_\alpha = 2\pi/L_\alpha$, N is the number of electrons, and $\text{Im} \ln z_\alpha$ is the phase of z_α . From Eq. 6 the remarkable result follows that, within PBC, the electronic polarization P is:

$$P_\alpha = \frac{2eN}{\Omega} \langle r_\alpha \rangle = -\frac{2e}{\Omega G_\alpha} \text{Im} \ln z_\alpha. \quad (7)$$

On the same footing, the electron localization, λ_α , (i.e. the spread of the single-particle position operator) can be calculated from the absolute value of z_N^α as:

$$\lambda_\alpha^2 = \langle r_\alpha^2 \rangle - \langle r_\alpha \rangle^2 = -\frac{1}{NG_\alpha^2} \ln |z_N^\alpha|^2. \quad (8)$$

Although Eqs.7 and 8 are valid for any system of interacting electrons, z_N^α is in practice calculated within the usual independent-particle approximation. Once the many-body wavefunction, Ψ_0 , is expressed as a single Slater determinant of Bloch wavefunctions we have that,³¹

$$z_N^\alpha = \det S_{n\mathbf{k},m\mathbf{k}'}^\uparrow \cdot \det S_{n\mathbf{k},m\mathbf{k}'}^\downarrow \quad (9)$$

where,

$$S_{n\mathbf{k},m\mathbf{k}'}^\uparrow = \langle \psi_{n\mathbf{k}}^\uparrow | e^{-i\Delta\mathbf{k}_\alpha \cdot \mathbf{r}} | \psi_{m,\mathbf{k}'}^\uparrow \rangle. \quad (10)$$

These are the elements of a $N^\uparrow \times N^\uparrow = (N_b^\uparrow M^3) \times (N_b^\uparrow M^3)$ matrix (N^\uparrow and N_b^\uparrow are the number of spin-up electrons and occupied bands, respectively). It is easy to see that they are only non-vanishing for $\mathbf{k}' = \mathbf{k} + \Delta\mathbf{k}_\alpha$. Thus the determinant in Eq.9 can be decomposed into a product of M^3 determinants (i.e. one for each point of the reciprocal space grid) of an $N_b^\uparrow \times N_b^\uparrow$ -dimensional matrix:

$$\det S_{n\mathbf{k},m\mathbf{k}'}^\uparrow = \prod_{\mathbf{k}} \det M_{n,m}^\uparrow(\mathbf{k}, \mathbf{k} + \Delta\mathbf{k}_\alpha), \quad (11)$$

where,

$$M_{n,m}^\dagger(\mathbf{k}, \mathbf{k} + \Delta\mathbf{k}_\alpha) = \left\langle \psi_{n,\mathbf{k}}^\dagger | e^{-i\Delta\mathbf{k}_\alpha \cdot \mathbf{r}} | \psi_{m,\mathbf{k}+\Delta\mathbf{k}_\alpha}^\dagger \right\rangle \quad (12)$$

A complication is caused by the use of USPP, since with the USPP method the Bloch states are not orthonormal, thus the expected value of the phase operator must be augmented by an additional term which restores the contribution of the augmented atomic charges, $q_{ij}(\mathbf{r})$'s. Thus, the following contribution $M_{n,m}^{US\uparrow}$ should be added to the matrix $M_{n,m}^\dagger$ given in Eq.12:

$$M_{n,m}^{US\uparrow}(\mathbf{k}, \mathbf{k} + \Delta\mathbf{k}_\alpha) = \sum_{i,j,l} \left\langle \psi_{n,\mathbf{k}}^\dagger | \beta_i^l \right\rangle \left\langle \beta_j^l | \psi_{m,\mathbf{k}+\Delta\mathbf{k}_\alpha}^\dagger \right\rangle \times e^{-i\Delta\mathbf{k}_\alpha \cdot \mathbf{R}_l} \int d\mathbf{r} q_{ij}(\mathbf{r}) e^{-i\Delta\mathbf{k}_\alpha \cdot \mathbf{r}}, \quad (13)$$

where \mathbf{R}_l are atomic positions.

The calculation of Eqs. 11, 12, and 13 is not demanding since the product over k-point space requires a dense grid only in the α -direction, whereas few k-points in the subspace orthogonal to α are generally sufficient to obtain a well-converged result for electron polarization and localization length along direction α .

III. RESULTS

A. Technicalities

Our local-spin density calculations²² are performed within a plane-wave basis set and employ ultra-soft pseudopotentials.²⁹ For the LDA calculations, Ti ($3s^2$), ($3p^6$) semi-core electrons are included as valence charge in order to improve the transferability of their respective pseudopotentials. This is not necessary in pseudo-SIC since these states are much lower in energy (see Ref.25 for a discussion about this point). In all cases we employ two beta functions for each angular channel. Also, non-linear core corrections have been used for all the atoms, and scalar-relativistic effects are included within the USPP for Ca, Ba, Ti, and Ge.

We use cut-off energies equal to 30 Ryd for CaMnO_3 and 40 Ryd for all the other compounds. For the calculation of the Berry phase, 6×6 special k-point grids are used for the integration in the plane orthogonal to the polarization direction, and up to 40 k-points to integrate along the parallel direction.

B. BaTiO_3 and GeTe

In this Section we investigate two ferroelectric materials. BaTiO_3 is one of the simplest and best known ferro-

electric perovskites, and the LDA successfully describes the energetics of the three ferroelectric phase transitions (tetragonal, orthorhombic and rhombohedral), provided that the experimental volumes are used for the calculations.³² The BEC values are also well-established by a long series of LDA calculations, and their large anomaly is assumed to be a major indication of ferroelectric instability. Also, the LDA calculations revealed that, despite the mainly ionic character of BaTiO_3 , some p-d hybridization is present,¹³ and the sensitivity of this hybridization to off-center atomic displacements is a fundamental force driving the system to the ferroelectric state.^{7,13} Despite these successes, the comparison between the LDA band-structure energies and the photoemission spectra³³ show typical discrepancies that are worthy of investigation.

In Figure IIIB (left panel) our calculated LDA band energies of cubic BaTiO_3 at the LDA volume are shown. The bands are well separated into groups, each with a single dominant orbital character. For the direct energy gap at Γ we obtain the value 1.94 eV (the absolute energy gap is indirect between R and Γ points and equal to 1.84 eV), in agreement with other LDA calculations,³⁴ while, as usual, the experiments indicate a much larger gap (3.2 eV³⁵). Also, the spread of the O p manifold is ~ 4.5 eV, in contrast to an experimental value of 5.5 eV.³³ Finally, the binding energies of the more localized, lowest-lying states (9.9 eV for the Ba 5p bands, 16.7 eV for the O 2s bands) are underestimated with respect to the corresponding photoemission energies (12.2 eV and 18.8 eV)

We see in the right panel of Figure IIIB that the pseudo-SIC repairs the LDA deficiencies to a large extent: The energy gap at Γ is 3.13 eV, the bandwidth of the O p manifold is ~ 6 eV, and the energies of Ba 5p and O 2s bands ~ 11.57 eV and 18 eV, respectively.

There is a long-standing debate³⁶ about the interpretation of the mismatch between the LDA (or LSDA) and the observed energy gap. Briefly, if the mismatch is attributed to the LDA inaccuracy, this may, in principle, affect any ground-state property. If otherwise the mismatch stems from a discontinuity of the exact energy functional (i.e. it depends on the DFT itself) it has no consequences on the ground-state properties. In fact, both these aspects contribute to the mismatch. In the present case, the agreement of pseudo-SIC and experimental energy gap is an indication that the LDA error is the dominant contribution.

In Table I the calculated values for the BEC are shown. The most important result is the remarkable decrease of Z^* for both Ti and O_T , when calculated within pseudo-SIC, with respect to their LDA counterparts. The pseudo-SIC values can still be described as anomalous if compared with the formal ionic charges, but the anomaly (1.88) is reduced by $\sim 40\%$ with respect to the LDA.

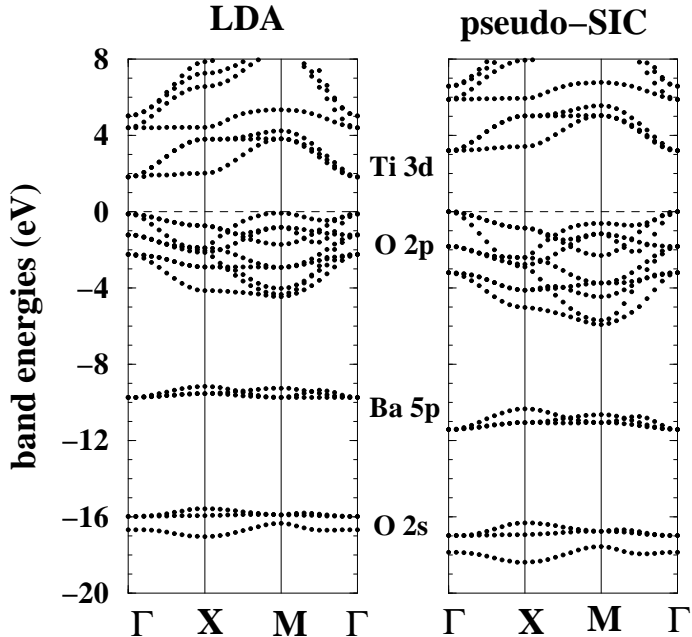


FIG. 1: Band structure of cubic BaTiO₃ calculated within LDA and pseudo-SIC.

TABLE I: Born effective charges, Z^* , and localization lengths, λ , (in Bohr) calculated within LDA and pseudo-SIC for cubic BaTiO₃. O_T and O_P label oxygens on-top of Ti and planar with Ti, respectively.

	Z_{Ba}^*	Z_{Ti}^*	$Z_{O_T}^*$	$Z_{O_P}^*$	λ
formal	2	4	-2	-2	
LDA	2.70	7.01	-5.54	-2.05	0.93
pseudo-SIC	2.61	5.88	-4.43	-2.03	0.97

This result may be expected since typically the SIC increases the removal energies and the space localization of the electron charges. This, in turn, reduces the overlap and the hybridization which is generally overemphasized within LDA.

In Table I the calculated localization lengths, λ , are also reported. In a many-body framework λ is an exact measure of the electron localization. In the one-electron approximation, it measures the average spatial localization of a single electron, thus it is a useful indicator of the overall metallic character of a system. The small value obtained for BaTiO₃ (less than 1 Bohr) is typical of highly ionic compounds (compare this, for example, with the values obtained for the series of III-V semiconductors in Ref.37). Also, notice that the LDA value is smaller than the pseudo-SIC result. This is caused by the presence of Ti 3s,3p semicore states in the LDA valence charge (these states are in the core for the SIC calcula-

TABLE II: Orbital occupation numbers for cubic BaTiO₃ calculated within LDA and pseudo-SIC. The numbers show the total orbital character for individual atoms. Ba s and p orbital occupations are relative to the low-lying semi-core states.

	LDA			pseudo-SIC		
	Ba	Ti	O	Ba	Ti	O
s	1.64	0.36	1.60	1.65	0.38	1.61
p	5.63	1.30	4.82	5.65	1.26	4.99
d t_{2g}	0.81	1.10		0.72	0.84	
d e_g	0.42	1.16		0.35	1.08	

tion). We will see later that, for the same valence states, the localization length is always smaller in pseudo-SIC.

The effect of the SIC on the orbital hybridizations can be appreciated in Table II where the orbital occupation numbers are reported. In pseudo-SIC the material is more ionic and the hybridizations between Ti d and O p orbitals are lowered. Indeed, in pseudo-SIC the Ti e_g , and t_{2g} , and the O p orbital occupations are closer to their respective nominal values.

Now we present our results for GeTe.^{38,39} This is an interesting ferroelectric since it possesses extremely anomalous BEC¹¹ and shows electronic properties markedly different from those of the most common ferroelectric perovskites. At high-temperature it has the rocksalt structure, and below $T_c \sim 650$ K³⁸ it undergoes a transition to a ferroelectric rhombohedral structure, with polarization parallel to the [111] axis.

In Figure III B the LSDA and pseudo-SIC band structures of rocksalt GeTe are shown. There are no d states or other highly localized states close to the energy gap region, and in fact the band structure shows fairly dispersed states both in the valence and in the conduction regions. Also, in this case LDA and pseudo-SIC give very similar results. This is consequence of the large hybridizations of the bands around the energy gap, with s and p orbital characters heavily mixed. When the bands are not dominated by a well-defined orbital character, or are not localized on a single atomic site, the SIC corrections over the LDA eigenvalues are small and mainly consist of a global shift in energy of the whole band manifold.⁴⁰

Due to the large band dispersion, GeTe is a quasi-metal, with a direct energy gap at $L=[1/2,1/2,1/2]$ $2\pi/a_0$ equal to 0.43 eV in LDA and 0.20 eV in pseudo-SIC. The metallicity is consistent with the huge LDA BEC value previously reported.¹¹ Our results give $Z_{\text{Te}} = -11.55$ electrons within LDA and $Z_{\text{Te}} = -8.27$ electrons in pseudo-SIC. Thus almost 35% of the LDA anomalous charge is actually due the SI error. The metallic character and the effect of the SIC can be quantitatively estimated from the values of the localization length. In LDA we obtain $\lambda = 2.81$ Bohr, a huge value in comparison to that the highly ionic BaTiO₃. This indicates the large (nearly metal-

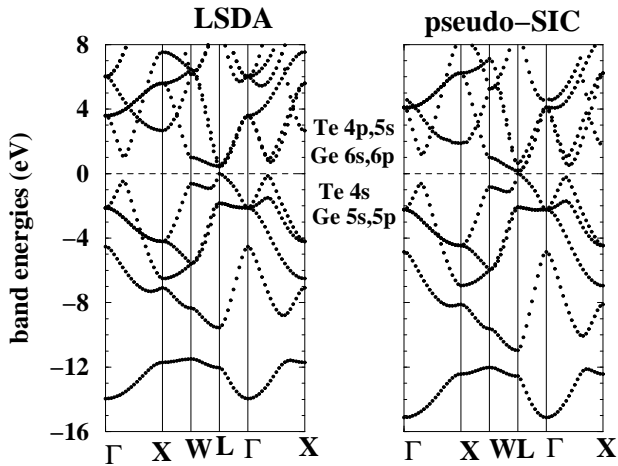


FIG. 2: Band structure of rock-salt GeTe calculated within LSDA and pseudo-SIC.

lic) spatial extension of the valence electron charges. In pseudo-SIC we have $\lambda = 2.47$ Bohr, (that is 23% smaller than the LDA value). The simultaneous decrease of λ and BEC obtained within pseudo-SIC is consistent with the idea that in the metallic limit, $\lambda = \infty$, the BEC calculated within the centrosymmetric structure should diverge.

To conclude this section we illustrate the mechanism of the anomalous currents in BaTiO₃ and GeTe by means of the simple scheme shown in Figure 3. Consider first the upper panel which refers to BaTiO₃. For simplicity, only Ti and O_T, which are the ions with the most anomalous BEC, are considered. Upon the Ti displacement (indicated by the arrow) a +4 ionic charge is transported upward. Simultaneously, a further electron current flows from the above oxygen towards the Ti, so that the positive charge effectively carried by the Ti along the displacement is larger than +4. Of course, the amount of the anomalous contribution depends on the detail of the energy spectrum, but we can make some considerations based on the capacity of the orbitals available to exchange charge. If we assume that the current can only flow from the highest occupied O orbitals to the lowest unoccupied Ti orbitals⁴¹, we can conclude by a simple criterion of orbital filling that the maximum value allowed for the anomalous contribution must be +8, that is (2s²)(2p²) oxygen electrons transferred to the 3d Ti orbitals, and than the largest BEC allowed according to this argument is 4+8 = +12 for Ti, and -2-8 = -10 for O_T. This criterion must hold for all the octahedrally-coordinated oxide perovskites with a d⁰ B-site transition metal, and indeed first-principle calculations support this prediction. See for example Ref.7 where a list of BEC for many ferroelectric perovskites is reported.

We can test the validity of this model for the IV-VI chalcogenides whose reported BEC are very anomalous,¹¹

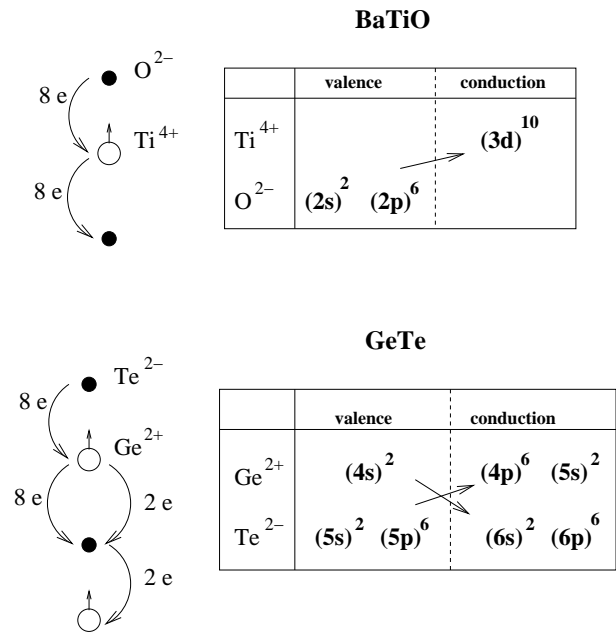


FIG. 3: Schematic diagram of anomalous charge flux in BaTiO₃ and GeTe. Small arrows indicate atomic displacements, long arrows show the directions of electron currents. For BaTiO₃ the anomalous charge can only flow from filled O 2s,2p to empty Ti 3d orbitals and amounts to a maximum of 8 electrons. For GeTe two channels are available, giving a total maximum current of 10 electrons. The calculated values are indeed below these maximum limits.

the biggest of whom is indeed found in GeTe. In order to justify the large value of the anomalous part (9.55 in our LDA calculation) we should consider that there are two available channels of electron current (shown in the lower panel of Fig.3): one involves the current from the filled Ge (4s)² to the empty Te (6s)², (6p)⁶ orbitals, and the other from the filled Te (5s)², (5p)⁶ to the empty Ge (4p)⁶, (5s)² orbitals. The sum of these two contributions give 10 electrons as a maximum limit of anomalous charge, which is indeed consistent with the calculated value.

C. CaMnO₃

In this Section we report our results for the G-type⁴² antiferromagnetic CaMnO₃.⁴³ Among the manganese perovskites, CaMnO₃ is the only compound stable in cubic symmetry since the Mn⁴⁺ ion has the three majority d t_{2g} orbitals fully occupied, and therefore does not undergoes Jahn-Teller distortions. Due to its formal ionic configuration Ca²⁺Mn⁴⁺O₃²⁻, this is the magnetic, non-ferroelectric perovskite which is better suited to be compared with BaTiO₃.

In a previous paper¹⁴ devoted to the analysis of orbital hybridizations we reported the fact that, within LSDA, CaMnO_3 shows anomalous BEC, with values similar to that of BaTiO_3 , and we argued that the BEC anomaly could be, in fact, a common characteristic of the whole family of perovskite oxides. However, the two materials show substantial differences in the electronic properties. BaTiO_3 is definitely more ionic in character, whereas CaMnO_3 show a larger band dispersion and hybridization. Furthermore, the small band gap obtained within LSDA for CaMnO_3 suggests that the large BEC could be due to an incipient insulator-metal transition. These facts motivated us to revisit the properties of CaMnO_3 within pseudo-SIC.

In Figure 4 we report the band structure calculations within LSDA and pseudo-SIC. Within pseudo-SIC the bands are flatter and spread over a wider energy range. In pseudo-SIC the valence band manifold of O 2p and Mn d t_{2g} states spans a region of 8 eV below the valence band top (VBT), where the same band manifold is 7 eV wide in LSDA. In both pseudo-SIC and LSDA the O 2s state are placed ~ 18 eV below the VBT. Within LSDA the fundamental energy gap is only 0.42 eV and occurs between points A= $[1/2, 1/2, 0]$ $2\pi/a$ (the VBT) and Γ , whereas within pseudo-SIC the gap is direct at Γ and equal to 1.88 eV. In both LSDA and pseudo-SIC the lowest group of conduction bands come from the majority e_g and the minority t_{2g} orbitals. (The t_{2g} bands are flatter and less hybridized than the e_g bands since they do not point towards the oxygens.)

Comparing these results with an x-ray absorption spectroscopy study⁴⁴ shows that the pseudo-SIC is in overall better agreement with experiment than LSDA. In particular, the pseudo-SIC reproduces well the observed distance between the average positions of the lowest conduction and highest valence bands (~ 3 eV), which is instead strongly underestimated in LSDA (~ 1.5 eV). Even the observed width of the O 2p-Mn t_{2g} occupied manifold (~ 9 eV) is in better agreement with the pseudo-SIC value, whereas both LSDA and pseudo-SIC correctly describe the material as a charge-transfer insulator (i.e. $U > \Delta$ in the language of Hubbard model⁴⁴).

On the basis of the energy band results, we expect that the BEC in pseudo-SIC should be markedly different from the LSDA values, and the results in Table III confirm this expectation: the values for Z_{Mn} and Z_{O_T} are reduced by $\sim 25\%$ in pseudo-SIC, although they still remain substantially anomalous. It is thus evident that part, but not all, of the BEC anomaly calculated in LSDA is due to the overestimation of the p-d hybridization. Furthermore, it is clear that anomalously large values of the BEC can be, as in this case, absolutely unrelated to any notion of ferroelectric behavior. (It is helpful to remember, indeed, that the energetics of CaMnO_3 , disfavours any ferroelectric distortion.¹⁴)

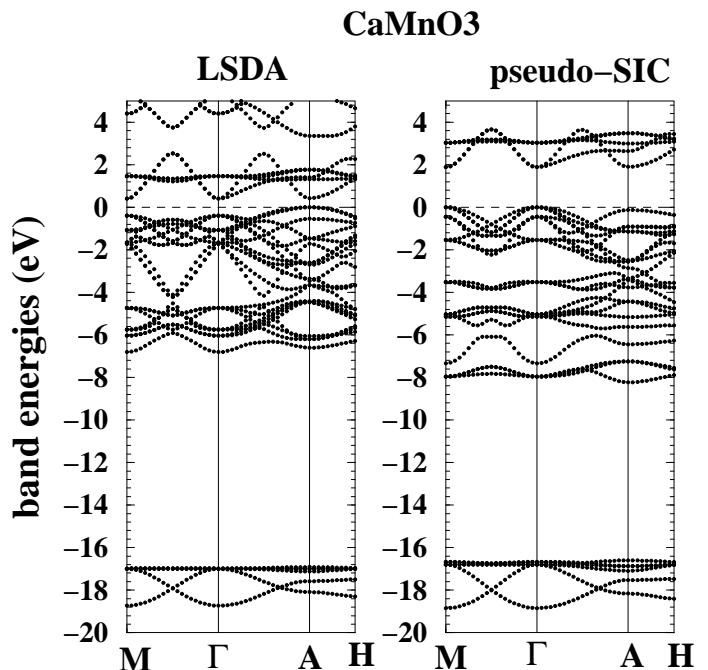


FIG. 4: Band energies for G-type AFM CaMnO_3 calculated within LSDA and pseudo-SIC.

TABLE III: Born effective charges for CaMnO_3 calculated within LSDA and pseudo-SIC. For Mn we also report the individual spin-up (Z_{Mn}^{\uparrow}) and spin-down ($Z_{\text{Mn}}^{\downarrow}$) electronic contributions. λ is the localization length (in Bohr).

	Z_{Ca}	Z_{Mn}	Z_{Mn}^{\uparrow}	$Z_{\text{Mn}}^{\downarrow}$	Z_{O_T}	Z_{O_P}	λ
formal	2	4	-3	0	-2	-2	
LSDA	2.74	7.60	-2.57	3.16	-6.75	-1.80	1.42
pseudo-SIC	2.87	6.03	-2.73	1.76	-5.36	-1.77	1.29

Finally, notice that, as in BaTiO_3 , the BEC for the A-site cation and O_P are slightly anomalous.

In Table III we also report the localization length. Within pseudo-SIC λ is smaller by $\sim 20\%$ than in LSDA, consistent with the reduction obtained for the BEC.

Finally, a fundamental question arises: how does the spin-polarization affect the values of the BEC? The total (i.e. spin-integrated) BEC does not contain the necessary information to answer this question. Thus, in Table III we show the electronic component of the Mn BEC decomposed into its spin-up and spin-down contributions (see Equation 9), so that:

$$Z_{\text{Mn}} = Z_{\text{Mn}}^{\text{ion}} + Z_{\text{Mn}}^{\uparrow} + Z_{\text{Mn}}^{\downarrow} \quad (14)$$

with $Z_{\text{Mn}}^{\text{ion}} = 7$. The result can be rationalized as fol-

lows: the majority contribution $Z_{\text{Mn}}^{el \uparrow}$ is substantially non-anomalous and close to its formal value -3. This means that the filled t_{2g}^{\uparrow} shell moves almost rigidly with the Mn^{7+} core. Instead, $Z_{\text{Mn}}^{el \downarrow}$ is highly anomalous. The t_{2g}^{\downarrow} states, which are at the bottom of the conduction band, can accept at most 3 electrons of anomalous current flowing from the O onto the Mn. In LSDA the energy separation between the center of the t_{2g}^{\downarrow} band manifold and the top of the O p valence bands is very small (~ 1 eV), thus the calculated anomalous, spin-down current (3.16) matches this acceptance limit (it is actually actually higher due to other secondary flux channels). Within pseudo-SIC, instead, the energy separation is ~ 3 eV, and the anomaly becomes drastically reduced to 1.76 electrons, that is almost half the LSDA value. On the other hand, the BEC contribution from the majority channel in pseudo-SIC is almost the same as in LSDA.

Notice that we do not show the separated spin-up and spin-down contributions for O since they are equal by symmetry.

In conclusion, in a magnetic material a correct interpretation of the BEC values can be only achieved if spin-up and spin-down components are disentangled, since their contribution to the integrated value can be highly anisotropic.

D. Transition-metal Monoxides

In this section we consider two magnetic, non-ferroelectric materials which are typical examples of systems for which the LSDA fails to give an accurate description, i.e. the AFM [111] A-type MnO and NiO.^{45,46,47} The band structures of these compounds within both LSDA and pseudo-SIC have been already presented in Ref.25, thus they will not be shown here. instead, here we briefly summarize the main conclusions of that investigation: Within LSDA the fundamental energy gaps (0.9 eV for MnO and 0.4 eV for Ni) are much smaller than the experimental values, and are of Mott-Hubbard type (i.e. the lowest energy excitation occurs between filled and empty d bands). Furthermore, the local magnetic moments ($4.42 \mu_B$ and $1.11 \mu_B$ for Mn and Ni, respectively) underestimate the measured values. The pseudo-SIC restores a good overall agreement between band energies and photoemission spectra: the energy gaps are 3.98 eV for MnO and 3.89 for NiO, the magnetic moments $4.71 \mu_B$ for Mn and $1.77 \mu_B$ for Ni, and the character of the energy gap is in the intermediate charge-transfer Mott-Hubbard regime, in agreement with experiments.

In Table IV the calculated values for the BEC and λ within LSDA and pseudo-SIC are shown. We first discuss MnO. Perhaps surprisingly after the strong differences described above for the band energy structures, the BEC

TABLE IV: Born effective charges for MnO and NiO calculated within LSDA and pseudo-SIC. The individual spin-up and spin-down electronic contributions are also shown. λ is the localization length (in Bohr).

MnO	Z_{Mn}	$Z_{\text{Mn}}^{el \uparrow}$	$Z_{\text{Mn}}^{el \downarrow}$	λ
formal	2	-5	0	
LSDA	2.31	-5.13	0.44	1.36
pseudo-SIC	2.29	-4.96	0.25	1.19
NiO	Z_{Ni}	$Z_{\text{Ni}}^{el \uparrow}$	$Z_{\text{Ni}}^{el \downarrow}$	λ
formal	2	-5	-3	
LSDA	2.31	-4.47	-3.22	1.18
pseudo-SIC	2.04	-4.87	-3.09	0.76

are found to be similar and substantially non anomalous within LSDA and pseudo-SIC (our LSDA result is in perfect agreement with an earlier linear-augmented plane waves calculation⁵⁰). This result can be understood from the band structures shown in Ref.25: MnO has, nominally, five fully occupied majority d bands and five empty minority d bands. In LSDA these two manifolds are separated by Hund's rule, whereas in pseudo-SIC the on-site Coulomb energy is dominant and the d-d energy gap increases dramatically. However, for this material the parameter which controls the anomalous charge is not the fundamental gap, but the energy separation between the highest occupied O p bands and the lowest unoccupied Mn d band. This is large (~ 4 eV) and similar in both LSDA and pseudo-SIC, thus the non-anomalous value for the BEC are justified.

Now consider the BEC decomposition within ionic and electronic, up-spin and down-spin components (Equation 14). The up-spin and down-spin formal charges are -5 and 0. We see that in LSDA both up-spin and down-spin electronic contributions are slightly anomalous, but the anomalies in the two channels have opposite signs (that is the currents flow in opposite directions) thus they cancel each other in the integrated value. The pseudo-SIC, in fact, reduces the anomalies in both channels, but, due to the current cancellations, this is not revealed in the total BEC which is indeed very close to the LSDA value.

For NiO we can repeat most of the considerations expressed for MnO. Now the energy gap in LSDA lies in the minority d band manifold and is due to the crystal field splitting which is only ~ 1 eV. This value underestimates by far the experimental value. However, as in MnO the p-d energy separation is ~ 4 eV and therefore no large anomalous charges contribute to the BEC. From the up-spin and down-spin decomposition (now $Z_{\text{Ni}}^{ion} = 10$) we see that there is also a cancellation between the corresponding anomalies. The cancellation is almost complete within pseudo-SIC, thus the BEC is almost equal to the formal value.

Finally, within pseudo-SIC we obtain a significant decrease of localization lengths for both these compounds with respect to the LSDA.

IV. DISCUSSION

Finally, we summarize the main findings of our analysis. We have seen that including strong-correlation effects within the band energy structure of strongly-correlated materials sensitively affects the values of the BEC and the electron localization lengths. With respect to the LDA or LSDA results, the pseudo-SIC systematically reduces both BEC and λ for all the investigated materials. This effect is particularly evident for materials with highly anomalous BEC (i.e. BaTiO₃ and CaMnO₃), and can be understood as resulting from the fact that the LSDA overemphasizes the orbital hybridizations and therefore the electron hopping. The decrease of electron localization lengths is also expected since the SIC enhances the binding energies and therefore the spatial localization of the electron charges. However, we point out that even within pseudo-SIC the anomalous contribution to the BEC is still substantial.

Our investigation reveals that the BEC are controlled by two fundamental parameters: one is the the energy separation between the highest occupied anionic bands and the lowest empty cationic bands. This criterion explains the trend of the BEC calculated for BaTiO₃ and CaMnO₃ (where the separation is less than 2 eV in LSDA and ~ 3 eV in pseudo-SIC) and the transition-metal mono-oxides, where it is ~ 4 eV in both LSDA and pseudo-SIC. The other important element is the metallic character of the system. It is very sound that in the metallic limit the BEC must be divergent, and the electron localization length gives us the possibility of evaluating this limit quantitatively. GeTe is a perfect material for such an analysis, since it is a ferroelectric with highly anomalous BEC and nearly metallic behavior. We found the GeTe energy gap small in both LDA and pseudo-SIC, but in pseudo-SIC both the localization length and the BEC are markedly smaller.

Finally, we should comment on the results of the two-band Hubbard model calculations,^{19,20} since our results are in contrast with these works, which predict that the introduction of the on-site Coulomb energy, U , should increase the BEC with respect to a single-particle scheme, and the BEC should undergo a sign change corresponding to the charge-transfer to Mott-Hubbard transition.

The disagreement is due to the fact that in the Hubbard model it is assumed that the on-site Coulomb energy of the anion favors a ground state with mixed anion-cation occupancy, instead of a purely anionic ground state. This causes, at large U , the transition from the charge-transfer to the Mott-Hubbard regime, and also

produces a sign change in the BEC since now the anomalous current can flow from the filled cation to the empty anion.

In density functional calculations what happens is quite the opposite: with the on-site Coulomb interaction on the ionic site turned on, a larger energy cost is associated with the fluctuation of the respective occupancy. The tendency to fluctuation is reduced by lowering (not raising) the energy of the filled anion bands. Thus, strong correlation effects further favor charge-transfer ground states over Mott-Hubbard regimes. This is in complete agreement with the photoemission spectroscopy data^{45,47} for transition-metal and perovskite oxides, as well as with the LDA+ U results.^{27,48,49} In conclusion, we think that the two-band Hubbard model is not adequate to describe materials like the ones studied in this paper, which present a complicated coexistence of charge localization and hybridization.

V. CONCLUSIONS

In this paper we revisited the behavior of the BEC by means of our recently proposed pseudo-SIC method which set the LSDA density functional free of the spurious SI, and thus describes the electronic properties of weakly as well as strongly correlated materials efficiently. We investigated two ferroelectric materials with highly anomalous BEC, and some magnetic materials with both anomalous and non-anomalous BEC.

Overall, we find that the anomalous part is systematically reduced (but not suppressed) by the SIC. The electron localization lengths is also reduced by the SIC, consistently with the idea that in the metallic limit the BEC must be divergent.

On the basis of these considerations, what can be argued about the BEC's ability to predict a ferroelectric instability? According to our results, there is no evidence to claim such a role for the BEC, since their values are related to features of the band energy spectrum which are not specifically properties of a ferroelectric material. We may argue that a compound with large BEC, if ferroelectric, will have a large spontaneous polarization, since this represents the integrated value of the BEC over the ferroelectric displacement,⁴ but the BEC value in itself is not indicative of, or specific to a chemical environment particularly favorable for non-ferroelectric-to-ferroelectric phase transition.

Acknowledgments

We thank Umesh Waghmare for many thoughtful discussions. We acknowledge financial support from the

National Science Foundation's Division of Materials Research under grant number DMR 00-80034. Most of the calculations have been carried out on the IBM SP2 ma-

chine of the MHPCC Supercomputing Center in Maui, HI.

-
- ¹ S. Baroni, P. Giannozzi, and A. Testa, *Phys. Rev. Lett.* **58**, 1861 (1987); X. Gonze, D. C. Allan, and M. P. Teter, *Phys. Rev. Lett.* **68**, 3603 (1992); X. Gonze, *Phys. Rev. B* **55**, 10337 (1997); X. Gonze and Ch. Lee, *Phys. Rev. B* **55** 10355 (1997).
- ² R. D. King-Smith and D. Vanderbilt, *Phys. Rev. B* **47**, 1651 (1993).
- ³ R. Resta, *Ferroelectrics* **136**, 51 (1992).
- ⁴ R. Resta, *Rev. Mod. Phys.* **66** 899 (1994).
- ⁵ W. Zhong, R. D. King-Smith, and D. Vanderbilt, *Phys. Rev. Lett.* **72**, 3618 (1994).
- ⁶ F. Bernardini, V. Fiorentini, and D. Vanderbilt, *Phys. Rev. B* **56**, R10024 (1977).
- ⁷ Ph. Ghosez, J.-P. Michenaud, and X. Gonze, *Phys. Rev. B* **58** 6224 (1998).
- ⁸ R. Resta, M. Posternak, A. Baldereschi, *Phys. Rev. Lett.* **70**, 1010 (1993).
- ⁹ M. Posternak, R. Resta, and A. Baldereschi, *Phys. Rev. B* **50** 8911 (1994).
- ¹⁰ Ph. Ghosez, X. Gonze, J.-P. Michenaud, *Ferroelectrics* **153**, 91 (1994).
- ¹¹ U. V. Waghmare, N. A. Hill, H. C. Kandpal, and R. Seshadri, *Phys. Rev. B*, to be published.
- ¹² R. E. Cohen and H. Krakauer, *Phys. Rev. B* **42**, 6416 (1990).
- ¹³ R. E. Cohen, *Nature* **358**, 136 (1992).
- ¹⁴ A. Filippetti and N. A. Hill, *Phys. Rev. B* **65**, 195120 (2002).
- ¹⁵ H. L. Yakel, W. C. Koehler, E. F. Bertaut, and E. F. Forrat, *Acta Cryst.* **16**, 957 (1963).
- ¹⁶ N. Fujimura, T. Ishida, T. Yoshimura, and T. Ito, *App. Phys. Lett.* **69**, 1011 (1996).
- ¹⁷ B. B. Van Aken, A. Meetsma, T. T. M. Palstra, *Acta Crystallogr., Sect. C: Cryst. Struct. Commun.* **57**, 230 (2001).
- ¹⁸ B. B. Van Aken, T. T. M. Palstra, A. Filippetti, N. A. Hill, to be published.
- ¹⁹ T. Egami, S. Ishihara, and M. Tachiki, *Science* **261**, 1307 (1993). S. Ishihara, T. Egami, and M. Tachiki, *Phys. Rev. B* **49**, 8944 (1994). S. Ishihara, M. Tachiki, and T. Egami, *Phys. Rev. B* **49**, 16123 (1994).
- ²⁰ R. Resta and S. Sorella, *Phys. Rev. Lett.* **74**, 4738 (1995).
- ²¹ R. Resta and S. Sorella, *Phys. Rev. Lett.* **82**, 370 (1999). For a comprehensive review, see also: R. Resta, *J. Phys. Condensed Matter* **14** R625 (2002).
- ²² J. P. Perdew and A. Zunger, *Phys. Rev. B* **23**, 5048 (1981).
- ²³ O. Gunnarsson, and R. O. Jones, *Phys. Rev. B* **31**, 7588 (1985).
- ²⁴ A. Svane, *Phys. Rev. Lett.* **68**, 1900 (1992); *ibid.* **72**, 1248 (1994).
- ²⁵ A. Filippetti and N. A. Spaldin, *Phys. Rev. B* **67**, 125109 (2003).
- ²⁶ D. Vogel, P. Krüger, and J. Pollmann, *Phys. Rev. B* **54**, 5495 (1996); *ibid.* **55**, 12836 (1997); *ibid.* **58**, 3865 (1998).
- ²⁷ V. I. Anisimov, J. Zaanen, and O. K. Andersen, *Phys. Rev. B* **44**, 943 (1991).
- ²⁸ A. B. Shick, A. I. Liechtenstein, and W. E. Pickett, *Phys. Rev. B* **60**, 10763 (1999).
- ²⁹ D. Vanderbilt, *Phys. Rev. B* **32**, 8412 (1985); K. Laasonen, A. Pasquarello, R. Car, Changyol Lee, and D. Vanderbilt, *Phys. Rev. B* **47**, 10142 (1993).
- ³⁰ R. Resta, *Phys. Rev. Lett.* **80**, 1800 (1998).
- ³¹ We use the fact that the overlap between two single Slater determinants equals the determinant of the matrix whose elements are overlaps of occupied Bloch states. Also, we assume that the Slater determinant do not couple spinors with different directions (thus, no spin-orbit interaction is present), so that up and down determinants can be factorized.
- ³² As usual, the volume calculated within LDA is too small. If the LDA volume is assumed, BaTiO₃ is not ferroelectric.
- ³³ L. T. Hudson, R. L. Kurtz, S. W. Robey, D. Temple, and R. L. Stockbauer, *Phys. Rev. B* **47**, 1174 (1993).
- ³⁴ Ph. Ghosez, X. Gonze, J.-P. Michenaud, *Europhys. Lett.* **33**, 713 (1996).
- ³⁵ S. H. Wemple, *Phys. Rev. B*, **2**, 2679 (1970).
- ³⁶ J. P. Perdew and M. Levy, *Phys. Rev. B* **56**, 16021 (1997), and references therein.
- ³⁷ C. Sgiaroviello, M. Peressi, and R. Resta, *Phys. Rev. B* **64**, 115202-1 (2001).
- ³⁸ K. M. Rabe and J. D. Joannopoulos, *Phys. Rev. B* **36**, 6631 (1987).
- ³⁹ J. Y. Raty *et al.*, *Phys. Rev. B* **65**, 115205-1 (2002).
- ⁴⁰ We point out that the pseudo-SIC does not account for genuine many-body corrections. For example in bulk silicon the band energies in pseudo-SIC are substantially identical to the bands calculated within LDA.
- ⁴¹ Indeed, this is a simplification since other orbitals such as Ba 5s and 5p furnish small contributions as well. See the band-by-band resolution for the BEC of BaTiO₃ calculated in Ref.7.
- ⁴² In the G-type configuration, all nearest-neighbor Mn have antiparallel spin allignment.
- ⁴³ For a recent review about CaMnO₃ see: *Physics of Manganites*, edited by T. A. Kaplan and S. D. Mahanti (Kluwer/Plenum, New York, 1999).
- ⁴⁴ G. Zampieri, F. Prado, A. Caniero, J. Briatico, M. T. Causa, M. Tovar, B. Alascio, M. Abbate, and E. Morikawa, *Phys. Rev. B* **58** 3755 (1998).
- ⁴⁵ K. Terakura, T. Oguchi, A. R. Williams, and J. Kübler, *Phys. Rev. B* **30**, 4734 (1984).
- ⁴⁶ G. A. Sawatzky and J. W. Allen, *Phys. Rev. Lett.* **53**, 2239 (1984).
- ⁴⁷ R. Zimmermann, P. Steiner, R. Claessen, F. Reinert, S. Hüfner, P. Blaha, and P. Dufek, *J. Phys. Cond. Mat.* **11**, 1657 (1999).
- ⁴⁸ I. V. Solov'yev and K. Terakura, *Phys. Rev. B* **58** 15496

(1998).
⁴⁹ O. Bengone, M. Alouani, P. Blöch, and J. Hugel, Phys. Rev. B **62** 16392 (2000).

⁵⁰ S. Massidda, M. Posternak, A. Baldereschi, and R. Resta, Phys. Rev. Lett. **82** 430 (1999).